Figure 1 shows how strongly the C4–C3–C2$^+$ angle influences the chemical shifts, particularly for C2$^+$, but also for C3 in **1**. When the C4 methyl is in a fully bridging position (68° CCC$^+$ angle) the chemical shifts of C2 and C3 become nearly equal (Figure 1 and Table II). Figure 1 also includes plots of data for the 1-propyl cation (summarized in Table II) constrained to various CCC$^+$ angles. The 1-propyl cation is not an experimentally observable species, but the IGLO results show that the influence of the degree of bridging on the local electronic environment of the cation center and adjacent nucleus appears to be general. The strong dependence on extent of bridging is also evident in the IGLO calculations for **3**, where a change of about 12° in CCC$^+$ angle produces a 56 ppm change at C2$^+$.

Previous IGLO calculations[10] on CH_3^+, and all secondary and tertiary carbocations calculated with classical geometries (from small ab initio basis sets), predict nearly identical carbon shifts of 360–370 ppm for C$^+$, which are far from the more shielded values of 320–340 ppm considered typical of classical cations.[11] However, very good matches of theoretical to experimental ^{13}C shifts for secondary and tertiary carbocations can be achieved following geometry optimizations with extended basis sets.[10] It is now clear that the strong dependence of the IGLO DZ calculated shifts on the basis sets used for geometry optimization is primarily due to the degree of bridging, since similar IGLO predictions (Table II) are obtained from 3-21G, 6-31G*, or MP2/6-31G* geometries, as long as the C–C–C$^+$ angle is similar. The lower levels of theory do not give fully optimized structures with enough bridging, by either carbon or hydrogen. Hence, even one of the simplest representatives of tertiary alkyl carbocations, the *tert*-pentyl cation, is not fully classical: partial bridging alters the local electronic structure sufficiently to shield C$^+$ and give the observed shift of 335.7 ppm. If there is any dynamic averaging in the *tert*-pentyl cation involving **2** and **3** as well as **1**, it is clear that the equilibrium must be dominated by partially bridged species to reach this observed shift.

The success of matching calculated and experimental chemical shifts, generally within ±10 ppm,[10] in part is its own justification for comparing theoretical (gas-phase) predictions with solution measurements. Further justification comes from the remarkable constancy shown by the chemical shifts of carbocations as long as the medium is sufficiently nonnucleophilic to support their existence. For example, an examination of the *tert*-pentyl cation prepared from the chloride in six different solvents of varying nucleophilicity and with both SbF_5 and AsF_5-based counterions found no evidence for nucleophilic interaction by solvent or counterion.[1d] The chemical shifts at all positions varied with conditions, but all variations were within a range of 2.5 ppm, and preparation from the alcohol in FSO_3H/SbF_5 gave similar shifts. The small shift variation at C$^+$ tracked very well with the changes at C$^+$ in the *tert*-butyl cation,[1d] so the variation cannot be attributed to varying populations of **1** and **2** with differential solvation. However, it is possible that solvation plays a role in the energy difference between **1** and **2** in solution. Solvent and counterion have been noted to have some influence on closely balanced structural equilibria in carbocations,[12] and NMR relaxation measurements suggest that solvation influences the rate of reorientation of carbocations in solution.[13]

The high sensitivity of the chemical shifts to the CCC$^+$ angle (ca. 6 ppm/deg from 68° to 98°) as shown in Figure 1 may also help explain observations of large intrinsic NMR isotope shifts in some carbocations upon substitution of deuterium for protium, particularly in those cases where partial bridging is well developed. For example, it was previously suggested that the large isotope shifts at C2$^+$ and C1 in the 2-methyl-2-norbornyl cation were due to perturbation of the degree of bending along the bridging coordinate for C2–C1–C6.[14] It is now obvious from Figure 1 that only slight changes in bond angles associated with bridging in carbocations produce large changes in chemical shifts.

Acknowledgment. This work was supported at Erlangen by the Stiftung Volkswagenwerk, the Fonds der Chemischen Industrie, and the Convex Computer Corporation. We also thank Prof. W. Kutzelnigg and his Bochum group particularly for the development of the IGLO program and Dr. M. Schindler for the Convex version. We also thank Prof. W. J. Hehre for providing facilities and advice and IBM Düsseldorf for providing computational facilities on which the higher level calculations were carried out. J.W.d.M.C. thanks CNPq-Brazil for financial support through a doctoral fellowship.

Supplementary Material Available: Table of the absolute energies of 2-methyl-2-butyl cation isomers and table of MP2-(FU)/6-31G* geometries (2 pages). Ordering information is given on any current masthead page.

(10) (a) Schindler, M. *J. Am. Chem. Soc.* **1987**, *109*, 1020. (b) Bremer, M.; Schleyer, P. v. R.; Schotz, K.; Kausch, M.; Schindler, M. *Angew. Chem.* **1987**, *99*, 795; *Angew. Chem., Int. Ed. Engl.* **1987**, *26*, 761. (c) Schleyer, P. v. R.; Laidig, K.; Wiberg, K. B.; Saunders, M.; Schindler, M. *J. Am. Chem. Soc.* **1988**, *110*, 300. (d) Laidig, K.; Saunders, M.; Wiberg, K. B.; Schleyer, P. v. R. *J. Am. Chem. Soc.* **1988**, *110*, 7652. (e) Bremer, M.; Schleyer, P. v. R.; Fleischer, U. *J. Am. Chem. Soc.* **1989**, *111*, 1147. (f) Koch, W.; Liu, B.; Schleyer, P. v. R. *J. Am. Chem. Soc.* **1989**, *111*, 3479. (g) Schleyer, P. v. R.; Koch, W.; Liu, B. Fleischer, U. *J. Chem. Soc., Chem. Commun.* **1989**, 1098. (h) Schleyer, P. v. R.; Carneiro, J. W. de M.; Koch, W.; Raghavachari, K. *J. Am. Chem. Soc.* **1989**, *111*, 5475. (i) Carneiro, J. W. de M.; Schleyer, P. v. R.; Koch, W.; Raghavachari, K. *J. Am. Chem. Soc.* **1990**, *112*, 4064.

(11) Kirchen, R. P.; Okazawa, N.; Ranganayakulu, K.; Rauk, A.; Sorensen, T. S. *J. Am. Chem. Soc.* **1981**, *103*, 597.

(12) (a) Kirchen, R. P.; Sorensen, T. S. *J. Am. Chem. Soc.* **1978**, *100*, 1487. (b) Kirchen, R. P.; Ranganayakulu, K.; Sorensen, T. S. *J. Am. Chem. Soc.* **1987**, *109*, 7811.

(13) Kelly, D. P.; Leslie, D. R. *J. Am. Chem. Soc.* **1990**, *112*, 9078.

(14) (a) Forsyth, D. A.; Botkin, J. H.; Puckace, J. S.; Servis, K. L.; Domenick, R. L. *J. Am. Chem. Soc.* **1987**, *109*, 7270. (b) Forsyth, D. A.; Panyachotipun, C. *J. Chem. Soc., Chem. Commun.* **1988**, 1564.

Direct Observation of Hot Vibrations in Photoexcited Deoxyhemoglobin Using Picosecond Raman Spectroscopy

Robert Lingle, Jr.,† Xiaobing Xu, Huiping Zhu, Soo-Chang Yu, and J. B. Hopkins*

Department of Chemistry, Louisiana State University Baton Rouge, Louisiana 70803

K. D. Straub

John L. McClellan VA Hospital Little Rock, Arkansas 72205

Received December 6, 1990

We present the first study of the hot vibrational population in a photoexcited heme protein *directly* observed in the picosecond anti-Stokes Raman spectrum. Time-resolved resonance Raman scattering selectively probes strongly enhanced vibrations of the porphyrin chromophore and provides specific information on the population of excited vibrations. Our pump–probe Raman experiment with 8-ps time resolution unambiguously detects the excited vibrational levels of deoxyhemoglobin (deoxyHb) which are populated following optical excitation. Assuming thermal distribution of vibrational energy, we estimate a vibrational temperature of 36 K above room temperature within our 8-ps resolution. The $1/e$ time constant for vibrational cooling is 2–5 ps.[1]

Several attempts have been made to characterize the ultrafast dynamics of vibrational energy dissipation in photoexcited heme proteins.[2-4] Previous Raman experiments were unable to probe

† Department of Physics and Astronomy, LSU.

(1) Picosecond dynamics data, to be published.

(2) Petrich, J. W.; Martin, J. L.; Houde, D.; Poyart, C.; Orzag, A. *Biochemistry* **1987**, *26*, 7914.

(3) Anfinrud, P. A.; Han, C.; Hochstrasser, R. M. *Proc. Natl. Acad. Sci. U.S.A.* **1989**, *86*, 8387.

0002-7863/91/1513-3992$02.50/0

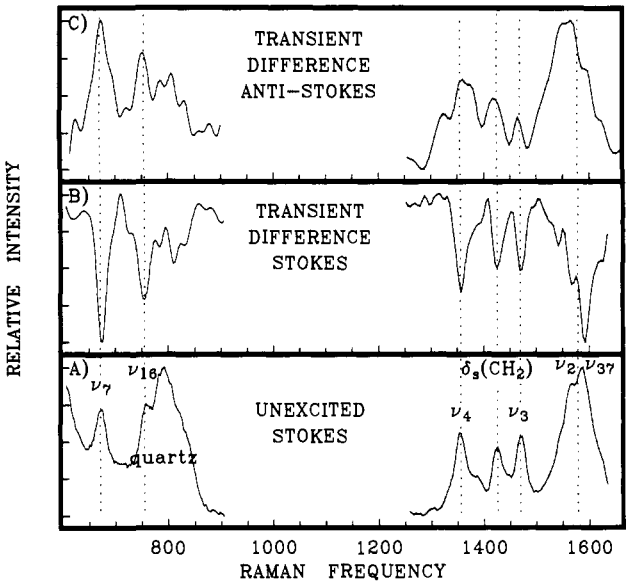

Figure 1. Resonance Raman spectra of deoxyHb in 100 mM phosphate buffer at pH 7.5. Part A shows the ground-state Stokes probe-only Raman spectrum. The marked bands are assigned[4,14-15] as ν_7 at 672 cm^{-1}, ν_{16} at 755 cm^{-1} (shoulder on quartz band), broad quartz window bands centered at 790 cm^{-1} (clearly labeled), weak ν_{32} on top of quartz bands at 790 cm^{-1}, ν_4 at 1359 cm^{-1}, a vinyl mode at 1430 cm^{-1}, ν_3 at 1475 cm^{-1}, and a broad group of overlapping bands including ν_2 plus ν_{37} plus others centered at 1580 cm^{-1}. Parts B and C show pure transient picosecond resonance Raman spectra obtained by subtracting 355-nm probe-only bands from the two-color spectrum. These spectra (B and C) show transient bands alone, with bands from unexcited molecules subtracted out. Part B shows depleted Stokes Raman scattering with the delay between 532-nm pump and 355-nm probe set at time zero. The Stokes negative transients are 6–8% of the corresponding unexcited band heights. Part C shows anti-Stokes Raman scattering at time zero. The positive anti-Stokes transient band height for ν_7 is ≈12% of the corresponding unexcited anti-Stokes band height (not shown). The positive anti-Stokes transient band height for ν_4 is ≈40% of the corresponding unexcited anti-Stokes band height (not shown). Positive anti-Stokes transient bands at the position of ν_7, ν_{16}, ν_4, the vinyl mode, ν_3, ν_2, and ν_{37} argue for Boltzmann distribution of heme internal modes, since all observed modes appear to be hot. Each of the six individual spectra are scaled independently to fill the height of the plot. Frequency units are in cm^{-1}. Unexcited spectra are not smoothed. Transient data have been minimally smoothed with Fourier transform filters ranging from three to six points.

the transient anti-Stokes spectrum and were interpreted by using indirect analyses. Knowledge of residual vibrational energy following photoexcitation is crucial when interpreting ultrafast dynamics. Our experiment is unique in that it *directly* and *unambiguously* detects hot vibrations in both low- and high-frequency porphyrin modes.

We have studied deoxyHb by exciting at 532 nm and probing at 355 nm. The experimental apparatus has been previously described in detail.[5,6] A pure transient resonance Raman spectrum is produced by subtracting the background probe-only components from the spectrum obtained with the pump–probe sequence.[7] The Stokes spectrum of Figure 1B shows a depletion of all ground-state Raman bands when the 532- and 355-nm pulses are temporally overlapped. The band assignments are given in the figure caption. The anti-Stokes spectrum in Figure 1C shows positive transient features at time zero. The observation of negative transient Stokes bands accompanied by positive anti-Stokes transient bands *cannot* be explained by shifts in the frequencies of the Raman bands resulting from structural changes in the heme. The negative/positive behavior of the Stokes/anti-Stokes transient spectrum is the unambiguous spectral signature of a vibrationally hot heme.

Picosecond transient absorption effects near the probe wavelength of 355 nm could alter deoxyHb Raman band intensities and might be confused with vibrational population relaxation. Transient absorption could arise from an electronically excited minority species[8,9] or from vibrational heating. Sulfate ion was added as a spectator Raman band to calibrate ultrafast absorbance changes in the sample. We find that transient absorption effects are at least nine times too weak to account for the transient Raman signals. Thus the deoxyHb Raman band dynamics are not primarily affected by transient absorption.[10]

Having eliminated transient absorption as the explanation for the data of Figure 1, we assign the dynamics in the vibrational spectra of parts B and C of Figure 1 to transient heating in the ground electronic state. The effect of vibrational population changes in the ground electronic state upon the Stokes and anti-Stokes Raman spectra can be understood as follows. Negative bands in the transient Stokes spectrum indicate less population in the vibrationless level of the photoexcited heme than for the unexcited molecule at room temperature.

Anti-Stokes scattering implies that the scattered photon withdraws a quantum of vibrational energy from the molecule. Our subtraction procedure removes all contributions of anti-Stokes scattering from levels thermally populated at room temperature. Clearly, a positive anti-Stokes transient signal indicates that photoexcited deoxyHb molecules are vibrationally hot. The complementary negative Stokes transient bands and positive anti-Stokes transient bands of Figure 1 are the predicted spectral signature of hot vibrations.

Our observation of vibrational heating is obvious from the form of the transient spectrum and does not rely on a temperature calculation. However, we can estimate the heme vibrational temperature by comparing the transient anti-Stokes signal at two delay times on two different Raman bands, specifically the ν_4 and ν_7 vibrations. We *assume* that the excess heat is distributed statistically among all modes on the time scale of our experiment[11-13] since all observed modes appear to be hot. The temperature is calculated by using the equation

$$\frac{H_4^*/H_4}{H_7^*/H_7} = \exp\left[\frac{E_4 - E_7}{k_B}\left(\frac{1}{T_{room}} - \frac{1}{T_{hot}}\right)\right]$$

H_n represents the unexcited anti-Stokes band intensity for mode n, while H_n^* represents the intensity of the photoexcited heme anti-Stokes band. The difference in resonance Raman enhancement for the two bands is factored out by the intensity ratios on the left-hand side of the expression. This calculation *does not* rely on an interpretation of the Stokes to anti-Stokes ratio of a particular resonance Raman band; rather it exploits the fact that we have measured the change in the anti-Stokes intensity of both a low- and a high-frequency Raman mode. The resulting estimate

(4) Alden, R. G.; Chavez, M. D.; Ondrias, M. R.; Courtney, S. H.; Friedman, J. M. *J. Am. Chem. Soc.* **1990**, *112*, 3241.
(5) Orman, L. K.; Chang, Y. J.; Anderson, D. R.; Yabe, T.; Xu, X.; Yu, S.-C.; Hopkins, J. B. *J. Chem. Phys.* **1989**, *90*, 1469.
(6) Chang, Y. J.; Xu, X.; Yabe, T.; Yu, S.-C.; Anderson, D. R.; Orman, L. K.; Hopkins, J. B. *J. Phys. Chem.* **1990**, *94*, 729.
(7) Lingle, R., Jr.; Xu, X.; Yu, S.-C.; Zhu, H.; Hopkins, J. B. *J. Chem. Phys.* **1990**, *93*, 5667.
(8) Cornelius, P. A.; Steele, A. W.; Chernoff, D. A.; Hochstrasser, R. M. *Chem. Phys. Lett.* **1981**, *82*, 9.
(9) Greene, B. I. *Chem. Phys. Lett.* **1985**, *117*, 2.
(10) We have also checked the temperature dependence of the absorption spectrum under equilibrium conditions. While the spectrum does change in the Soret region, the absorbance change at 354.7 nm is only 0.2% for a 15 K temperature jump.
(11) This is an assumption, but it is a reasonable and credible assumption for an 8-ps laser pulse. Previous studies of large molecules in the condensed phase indicate that IVR takes ≈1 ps (see: *Chem. Phys. Lett.* **1984**, *104*, 121; **1985**, *119*, 259). Asher and Murtaugh (*J. Am. Chem. Soc.* **1983**, *105*, 7244) and Petrich et al.[2] have demonstrated that ν_4 and many bands in the 1550–1650-cm^{-1} region of our spectrum are anharmonically coupled to low-frequency modes. Such modes are unlikely places for vibrational energy to hang up.
(12) Henry, E. R.; Eaton, W. A.; Hochstrasser, R. M. *Proc. Natl. Acad. Sci. U.S.A.* **1986**, *83*, 8982.
(13) Dlott, D. D. *J. Opt. Soc. Am. B* **1990**, *7*, 1638.
(14) Choi, S.; Spiro, T. G. *J. Am. Chem. Soc.* **1983**, *105*, 3683.
(15) Choi, S.; Spiro, T. G.; Langry, K. C.; Smith, K. M.; Budd, D. L.; LaMar, G. N. *J. Am. Chem. Soc.* **1982**, *104*, 4345.

is 36 K above room temperature, with a worst case lower limit of 12 K and an upper limit of 63 K. This estimate is not needed to support the observation of cooling but is useful as an indication that we are observing the later stages of cooling within our 8-ps laser pulse. The 532-nm photon causes a 460 K temperature jump.[12] Within 8 ps, most of the cooling is over. However, the molecule is still vibrationally hot and relaxes with a 2-5-ps $1/e$ time constant.[1]

Anatomy of a Stable Intramolecularly Hydrogen Bonded Folding Pattern†

Gui-Bai Liang, Gregory P. Dado, and Samuel H. Gellman*

S. M. McElvain Laboratory of Organic Chemistry
Department of Chemistry, University of Wisconsin
1101 University Avenue, Madison, Wisconsin 53706

Received December 27, 1990

We recently reported that triamide **1** exists predominantly in the intramolecularly hydrogen bonded folding pattern **1a** in nonpolar and moderately polar solvents (CH_2Cl_2 and CH_3CN) at room temperature.[1] The stability of form **1a** is remarkable in light of the molecule's inherent conformational flexibility; formation of the internal hydrogen bond restricts rotations about one C–N and three C–C single bonds. We now describe a series of experiments that elucidates the origin of this folding pattern's stability. These studies are part of our continuing effort to understand, from the physical organic chemist's perspective, the interplay of noncovalent forces that controls protein folding patterns.[1-3]

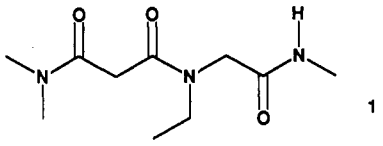

1

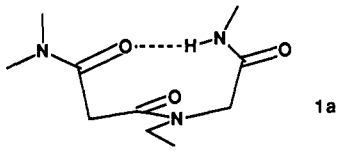

1a

Diamide **2** has available to it a nine-membered-ring hydrogen bond similar to the one that occurs in **1**, but as we have previously shown, **2** experiences little internal hydrogen bonding in CH_2Cl_2 or CH_3CN at room temperature.[2] Diamide **2** is more flexible than **1**, because the central, rotationally restricted C–N bond in **1** is replaced with an sp^3–sp^3 C–C bond in **2**. We prepared diamide **3**[4] in order to determine whether simply abolishing rotation about the central bond of the covalent skeleton would stabilize the internally hydrogen bonded state. FT-IR analysis of **3** (10 mM in CH_3CN) reveals that the trans double bond does not substantially stabilize the folded state. Under these conditions, the N–H stretch regions for **2** and **3** are quite similar, showing only one distinct band, at about 3400 cm^{-1}, indicating hydrogen bonding to the solvent.[2b] In contrast, triamide **1** in CH_3CN shows a

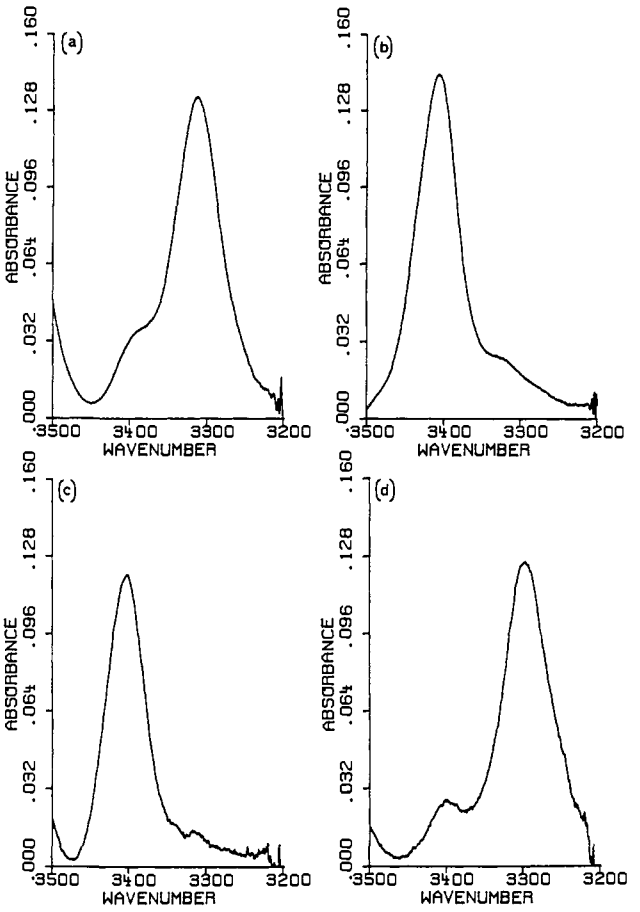

Figure 1. N–H stretch region FT-IR spectra for 10 mM amide solutions in CH_3CN (room temperature), after subtraction of the spectrum of pure CH_3CN. Data obtained on a Nicolet 740 spectrometer: (a) triamide **1** (maximum at 3313 cm^{-1}); (b) diamide **2** (maximum at 3406 cm^{-1}); (c) diamide **3** (maximum at 3403 cm^{-1}); (d) diamide **7** (maximum at 3298 cm^{-1}).

dominant band at 3313 cm^{-1}, indicating an intramolecular N—H···O=C interaction (Figure 1a–c).

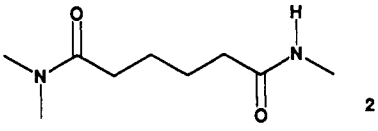

2

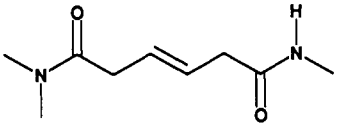

3

The behavior of **3** caused us to wonder whether the central amide group of **1** stabilizes the folded conformation by participating in a bifurcated hydrogen bond (**1b**). This uncertainty could

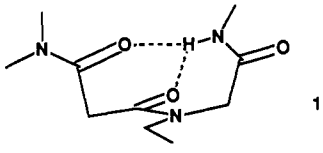

1b

by resolved by comparing the amide I regions of the IR spectra of **1** and methylated derivative **4**,[4] since hydrogen-bond acceptance by a carbonyl shifts the amide I band (largely C=O stretch) to lower wavenumber. These experiments required samples of **1** and **4** selectively labeled with ^{13}C, in order to eliminate band overlap. The positions of the amide I bands (cm^{-1}) are shown in the following structures (an asterisk indicates ^{13}C labeling; all samples 1 mM in CH_2Cl_2). Replacing the lone amide proton of **1** with

† Dedicated to Professor Ronald Breslow on the occasion of his 60th birthday.

(1) (a) Gellman, S. H.; Adams, B. R.; Dado, G. P. *J. Am. Chem. Soc.* **1990**, *112*, 460. (b) Dado, G. P.; Desper, J. M.; Gellman, S. H. *J. Am. Chem. Soc.* **1990**, *112*, 8630.

(2) (a) Gellman, S. H.; Adams, B. R. *Tetrahedron Lett.* **1989**, *30*, 3381. (b) Gellman, S. H.; Dado, G. P.; Liang, G.-B.; Adams, B. R. *J. Am. Chem. Soc.* **1991**, *113*, 1164.

(3) For a recent review on the role of noncovalent interactions in determining protein folding patterns, see: Dill, K. A. *Biochemistry* **1990**, *31*, 7133.

(4) The covalent structures assigned to all new compounds are consistent with NMR, IR, and MS analysis. Synthetic routes and full characterization will be reported elsewhere.

0002-7863/91/1513-3994$02.50/0